Journal of Medicinal Chemistry Article

J. Med. Chem. **2010,** *53,* 7825–7835 **7825**
DOI: 10.1021/jm100977d

Fruitful Adrenergic α_{2C}-Agonism/α_{2A}-Antagonism Combination to Prevent and Contrast Morphine Tolerance and Dependence[1,†]

Fabio Del Bello,[‡] Laura Mattioli,[‡] Francesca Ghelfi,[‡] Mario Giannella,[‡] Alessandro Piergentili,[‡] Wilma Quaglia,[‡] Claudia Cardinaletti,[‡] Marina Perfumi,[‡] Russell J. Thomas,[§] Ugo Zanelli,[§] Carla Marchioro,[∥,⊥] Michele Dal Cin,[∥,⊥] and Maria Pigini*,[‡]

[‡]*Scuola di Scienze del Farmaco e dei Prodotti della Salute, Università di Camerino, via S. Agostino 1, 62032 Camerino, Italy,* [§]*Siena Biotech SpA, Strada del Petriccio e Belriguardo 35, 53100 Siena, Italy, and* [∥]*GlaxoSmithKline Medicines Research Center, via Fleming 4, 37135 Verona, Italy.* [⊥]*Current address: Aptuit Verona, via Fleming 4, 37135 Verona, Italy*

Received July 30, 2010

The functional in vitro study of the enantiomers of imidazolines **4**−**7** highlighted the role played by the nature of the ortho phenyl substituent in determining the preferred α_{2C}-AR configuration. Indeed, the (*S*) enantiomers of **4**−**6** or (*R*) enantiomer of **7** behave as eutomers and activate this subtype as full agonists; the corresponding distomers are partial agonists. Because in clinical pain management with opioids α_{2C}-AR agonists, devoid of the α_{2A}-AR-mediated side effects, may represent an improvement over current therapies with clonidine like drugs, **4** and its enantiomers, showing α_{2C}-agonism/α_{2A}-antagonism, have been studied in vivo. The data suggest that partial α_{2C}-activation is compatible with effective enhancement of morphine analgesia and reduction both of morphine tolerance acquisition and morphine dependence acquisition and expression. On the contrary, full α_{2C}-activation appears advantageous in reducing morphine tolerance expression. Interestingly, the biological profile displayed by **4** (allyphenyline) and its eutomer (*S*)-(+)-**4** has been found to be very unusual.

Introduction

α_2-Adrenoreceptors (α_2-ARs[a]), belonging to the superfamily of G-protein coupled receptors,[2] consist of three subtypes (α_{2A}, α_{2B}, and α_{2C}) and are considered attractive therapeutic targets for the treatment of a wide range of diseases.[3] Because of the lack of α_2-AR subtype selective agonists, the attribution of physiological functions to a given α_2-AR subtype has proven challenging in vivo. Although genetic manipulations present some limitations, the use of mice carrying the D79N α_{2A}-AR, mice that are singly (α_{2A}-AR$^{-/-}$, α_{2B}-AR$^{-/-}$, α_{2C}-AR$^{-/-}$), doubly (α_{2AC}-AR$^{-/-}$), or triply (α_{2ABC}-AR$^{-/-}$) deficient in a particular subtype, or mice overexpressing the α_{2C}-AR (α_{2C}-AR$^{+/+OE}$) yielded important information about the subtype-specific functions.[4] These studies demonstrated that α_{2A}-AR subtype mediates hypotension, sedation, analgesia, hypothermia, antiepileptogenesis, and inhibition of monoamine release and metabolism in the brain. The α_{2B} subtype mediates hypertension and initial peripheral hypertensive responses to α_2-AR agonists. Finally, the α_{2C}-AR subtype appears to be involved in many CNS processes, such as the startle reflex, stress response, and locomotion as well as feedback inhibition of adrenal catecholamine release. Moreover, it has been highlighted that the α_{2C} subtype can contribute to adrenergic opioid synergy and spinal α_2-agonist-mediated analgesia.[5] The discovery and the development of ligands endowed with preferential α_2-AR recognition and able to produce individual subtype activation have been the focus of our research over the years.[6] Our studies demonstrated that conservative chemical modifications in the aromatic moiety (Ar) of the α_2-AR antagonist **1** (Chart 1, Table 1), which lacks subtype selectivity, caused an important modulation of receptor interaction and also affected the subtype selectivity. Indeed, the introduction of a pendant phenyl substituent into the ortho position provided the interesting α_{2A}- and α_{2C}-AR agonist biphenyline (**2**). Its enantiomer, (*S*)-(−)-**2**, was endowed with enhanced long-lasting antinociceptive potency.[7,8]

Chart 1

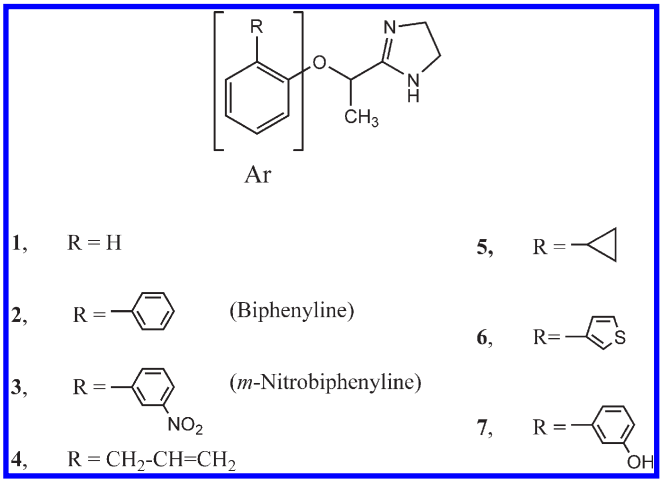

[†]This article is dedicated to the memory of Dr. Hervé Paris.

*To whom correspondence should be addressed. Phone: +39 0737 402257. Fax: +39 0737 637345. Email: maria.pigini@unicam.it.

[a] Abbreviations: α_2-ARs, α_2-adrenoreceptors; DEAD, diethyl azodicarboxylate; [(+)-(*R*)-MTPA], (*R*)-(+)-α-methoxy-α-(trifluoromethyl)phenylacetic acid; ADME, absorption, distribution, metabolism, excretion; PAMPA, parallel artificial membrane permeability assay; CHO, chinese hamster ovary; MDCK, Madin Darby Canine Kidney cell line.

Published on Web 10/06/2010

Table 1. Affinity (pK_i[a]), Antagonist Potency (pK_b[b]), Agonist Potency (pEC_{50}[b]), and Intrinsic Activity (ia[b]) on Human α_2-AR Subtypes

	α_{2A}			α_{2B}			α_{2C}		
compd	pK_i	pEC_{50} (pK_b)	ia	pK_i	pEC_{50} (pK_b)	ia	pK_i	pEC_{50} (pK_b)	ia
1	7.57 ± 0.09	(7.01 ± 0.10)		6.78 ± 0.13	(6.20 ± 0.18)		6.58 ± 0.12	(6.85 ± 0.15)	
(±)-**2** biphenyline	7.32 ± 0.08	6.94 ± 0.06	0.70	6.30 ± 0.07	6.19 ± 0.01	0.50	6.70 ± 0.04	7.24 ± 0.01	0.80
(*R*)-(+)-**2**	6.73 ± 0.04	4.54 ± 0.07	0.40	5.90 ± 0.03	4.00 ± 0.05	0.40	6.01 ± 0.05	6.95 ± 0.08	0.70
(*S*)-(−)-**2**	7.04 ± 0.08	7.13 ± 0.03	0.80	6.23 ± 0.08	6.16 ± 0.10	0.65	6.52 ± 0.09	7.73 ± 0.14	0.90
(±)-**3***m*-nitrobiphenyline	7.22 ± 0.03	(6.80 ± 0.05)[c]		6.18 ± 0.08	(5.90 ± 0.10)[c]		6.63 ± 0.08	7.00 ± 0.09	0.60
(*R*)-(+)-**3**	7.09 ± 0.08	(7.11 ± 0.15)		6.13 ± 0.07	(6.07 ± 0.09)		6.59 ± 0.09	8.00 ± 0.04	0.80
(*S*)-(−)-**3**	7.14 ± 0.06	(7.35 ± 0.16)		5.80 ± 0.06	(5.93 ± 0.12)		6.27 ± 0.08	6.13 ± 0.01	0.45
(±)-**4**	7.24 ± 0.11	(7.40 ± 0.06)		6.47 ± 0.20	NA		7.07 ± 0.14	7.30 ± 0.09	0.90
(*R*)-(−)-**4**	7.00 ± 0.08	(7.40 ± 0.09)		6.25 ± 0.12	NA		6.75 ± 0.11	6.73 ± 0.11	0.50
(*S*)-(+)-**4**	7.28 ± 0.05	(7.80 ± 0.13)		6.40 ± 0.09	6.00 ± 0.09	0.65	7.15 ± 0.09	7.60 ± 0.14	0.90
(±)-**5**	7.64 ± 0.20	(7.00 ± 0.09)		6.51 ± 0.13	5.50 ± 0.15	0.70	7.10 ± 0.16	7.40 ± 0.13	0.90
(*R*)-(−)-**5**	7.35 ± 0.10	(6.90 ± 0.07)		6.25 ± 0.10	NA		6.90 ± 0.13	6.90 ± 0.12	0.50
(*S*)-(+)-**5**	7.68 ± 0.12	(7.70 ± 0.11)		6.58 ± 0.08	5.50 ± 0.13	0.65	7.20 ± 0.10	7.45 ± 0.16	0.90
(±)-**6**	7.34 ± 0.02	7.12 ± 0.08	0.70	6.38 ± 0.04	NA		6.88 ± 0.07	7.03 ± 0.28	0.85
(*R*)-(−)-**6**	6.78 ± 0.13	5.50 ± 0.09	0.40	6.15 ± 0.07	NA		6.50 ± 0.12	7.00 ± 0.21	0.70
(*S*)-(+)-**6**	7.35 ± 0.08	7.20 ± 0.13	0.80	6.35 ± 0.12	6.00 ± 0.11	0.60	6.90 ± 0.08	8.20 ± 0.18	0.90
(±)-**7**	7.56 ± 0.02	(6.20 ± 0.11)[c]		6.45 ± 0.01	5.28 ± 0.17	0.50	7.75 ± 0.08	7.33 ± 0.15	1.15
(*R*)-(+)-**7**	7.40 ± 0.09	(6.40 ± 0.08)		6.50 ± 0.04	(5.67 ± 0.12)		7.50 ± 0.10	7.60 ± 0.11	1.00
(*S*)-(−)-**7**	7.01 ± 0.07	(6.00 ± 0.12)		6.00 ± 0.09	(5.50 ± 0.10)		6.95 ± 0.11	5.60 ± 0.09	0.65
clonidine		8.08 ± 0.12	0.90		5.93 ± 0.27	0.45		7.24 ± 0.14	0.60

[a] pK_i values were calculated from [^{3}H]RX 821002 on membrane preparations from CHO cells expressing individually each human α_2-AR subtype (α_{2A}, α_{2B}, α_{2C}). [b] pK_b, pEC_{50} and intrinsic activity (ia) values were determined by applying the Cytosensor microphysiometry system to the same cell models. Intrinsic activity of the tested compounds is expressed as the fraction of that of the full agonist (−)-noradrenaline taken as equal to 1. The data are expressed as means ± SEM of three−six separate experiments. Compounds exhibiting ia of < 0.3 were considered not active (NA). [c] Determined in the present study.

The further insertion of polar functions into the meta position of the pendant phenyl substituent induced a significant and selective α_{2C}-AR activation (for example *meta*-nitrobiphenyline, **3**)[8] (Chart 1, Table 1). This biological profile modulation from antagonist to agonist was attributed to the favorable interaction of the ortho pendant substituent with the amino acid residues comprising the highly conserved aromatic cluster (defined by Trp6.48, Phe6.51, and Phe6.52) of the sixth transmembrane domain of the α_2-AR cavity.[8,9] Subsequent studies also demonstrated that the effects found for the ortho phenyl substituent were also induced by its oximino-methyl bioisoster, whereas cyclopentyl and cyclohexyl groups triggered indiscriminate activation of all three α_2-AR subtypes.[10] The introduction in the Ar group of ortho substituents characterized by moderate steric hindrance, such as allyl or cyclopropyl groups, induced modulation of the biological profile of the antagonist **l**, only at α_{2C}-AR subtype,[6,10] similarly to what observed for **3**. Indeed, compounds **4** and **5** were potent and selective α_{2C}-agonists, while efficiently antagonizing the α_{2A}-AR subtype (Chart 1, Table 1). Also **3** and its enantiomers[11] activated the α_{2C}- and simultaneously antagonized especially the α_{2A}-AR subtype (Table 1), but unlike **4** and **5**,[6] they proved able to interact with good affinity with the α_{1a}-AR subtype (pK_i values between 7.0 and 7.8); their affinity for α_{1b}- and α_{1d}-AR subtypes is negligible (data not published). On the basis of the assumption that in clinical pain management, α_{2C} selective agonists, devoid of the sedative side effects associated with α_{2A}-AR stimulation, might represent alone or in combination with opioid analgesics an improvement over current therapies with clonidine-like drugs, **4** and **5** coadministered with morphine were tested in the algesiometric paradigm mouse tail-flick test.[6] From in vivo dose−response studies, it emerged that the low experimental dose (0.05 mg/kg) of both compounds caused a significant increase in morphine analgesia and this effect was comparable to that obtained with 0.5 mg/kg dose of clonidine. The potentiation of opioid analgesia displayed by **4** and **5** confirmed previous results obtained from genetically engineered mice.[5] In addition, at doses producing significant morphine analgesia enhancement, **4** and **5** were devoid of sedative side effects.[6] To increase our understanding of the interesting biological profile of these compounds, an assessment of the physicochemical and in vitro ADME properties of **4** was determined. Additionally, the presence of a stereocenter in **4** and **5** prompted us to investigate the stereochemical requirements for a possible improvement of their biological profile. Therefore, both enantiomers of **4** and **5** were prepared and evaluated by binding and functional assays on CHO cells expressing recombinant human α_2-AR and α_1-AR subtypes. Because the lipophilic (π) and electronic (σ) effects of the ortho phenyl substituent might contribute in determining the preferred α_2-AR subtype configurations, for a useful comparison, we also included in this investigation the preparation and in vitro study of the enantiomeric pairs of **6** and **7**[8] (Chart 1). For the in vivo study, the modulation of morphine analgesia on mouse tail-flick test was evaluated at the dose of 0.05 mg/kg for both enantiomeric pairs of **4** and **5**. In addition, the effects of **4** and its enantiomers on the acquisition and expression of morphine tolerance and dependence were determined; also these experiments were carried out at the dose of 0.05 mg/kg.

Chemistry

The enantiomers (*S*)-(+)- and (*R*)-(−)-**4**, (*S*)-(+)- and (*R*)-(−)-**5**, and (*S*)-(+)- and (*R*)-(−)-**6** were prepared according to Scheme 1. (*S*)-(−)- and (*R*)-(+)-2-(2-Allylphenoxy)propionic acid methyl ester [(*S*)-(−)-**8** and (*R*)-(+)-**8**, respectively], (*S*)-(−)- and (*R*)-(+)-2-(2-cyclopropylphenoxy)propionic acid methyl ester [(*S*)-(−)-**9** and (*R*)-(+)-**9**, respectively], and (*S*)-(+)- and (*R*)-(−)-2-(2-thiophen-3-yl-phenoxy)-propionic acid methyl ester [(*S*)-(+)-**10** and (*R*)-(−)-**10**, respectively] were obtained by Mitsunobu reaction from the appropriate phenol[12,13] and methyl (*R*)-(+)- or (*S*)-(−)-lactate, respectively, with inversion of configuration.[14] The reaction of (*S*)-(−)-**8**, (*S*)-(−)-**9**, (*S*)-(+)-**10**, (*R*)-(+)-**8**, (*R*)-(+)-**9**, or (*R*)-(−)-**10**

with ethylenediamine in the presence of $(CH_3)_3Al$ yielded the corresponding imidazolines (*S*)-(+)-**4**, (*S*)-(+)-**5**, (*S*)-(+)-**6**, (*R*)-(−)-**4**, (*R*)-(−)-**5**, and (*R*)-(−)-**6**, whose enantiomeric purity, determined by ^{1}H NMR spectroscopy or HPLC, was <98%. Therefore, the two (*S*)-(+)-**6** and (*R*)-(−)-**6** enantiomers were subsequently resolved by fractional crystallization of the hydrogen dibenzoyl-L- and hydrogen dibenzoyl-D-tartrate salts, respectively. The enantiomeric purity of amines (*S*)-(+)-**6** and (*R*)-(−)-**6**, determined by HPLC of their corresponding diastereomeric ureidic derivatives **11** and **12**, obtained by reaction with (*R*)-(+)-α-methylbenzyl isocyanate, was found to be >98% (detection limit). The enantiomeric purity was further confirmed by ^{1}H NMR spectroscopy in the presence of the chiral shift reagent (*S*)-(+)-2,2,2-trifluoro-1-(9-anthryl)-ethanol. In fact, the ^{1}H NMR spectrum of racemic compound (±)-**6** showed a double doublet at δ 1.44 ppm for the methyl protons, whereas only one doublet was observed for (*R*)-(−)-**6** and (*S*)-(+)-**6** at δ 1.44 and δ 1.46 ppm, respectively. Attempts to obtain the pure enantiomers (*S*)-(+)-**4**, (*S*)-(+)-**5**, (*R*)-(−)-**4**, and (*R*)-(−)-**5** by fractional crystallization were unsuccessful. Therefore, resolution of the racemic imidazolines (±)-**4** and (±)-**5**[6] was performed by HPLC using Chiralcel OD-H (25 cm × 0.46 cm) as the chiral stationary phase and *n*-hexane/2-propanol 90/10 v/v or *n*-hexane/2-propanol 85/15 v/v as the mobile phase for (±)-**4** and (±)-**5**, respectively (Figure 1). The enantiomeric purity of amines (+)-**4**, (−)-**4**, (+)-**5**, and (−)-**5**, determined by HPLC and further confirmed by ^{1}H NMR spectroscopy in comparison with the spectra of racemic compounds (±)-**4** or (±)-**5** and on addition of the chiral shift reagent (*S*)-(+)-2,2,2-trifluoro-1-(9-anthryl)-ethanol, was found to be >98% (detection limit) for all enantiomers. In fact, the spectrum of (±)-**4** showed a double doublet at δ 1.34 ppm for the methyl protons, whereas only one doublet was observed for (+)-**4** and (−)-**4** at δ 1.32 and δ 1.36 ppm, respectively. Similarly, for the enantiomers (+)-**5** and (−)-**5**, one doublet was observed at δ 1.44 and δ 1.40 ppm, respectively, whereas in the spectrum of (±)-**5**, the double doublet for the methyl protons was at δ 1.42 ppm.

The absolute configuration of the stereocenter in the bridge of enantiomers (+)-**4** and (+)-**5** was determined by comparing the sign of their optical rotations with those of the enantiomers obtained by stereospecific synthesis. Consequently, an *S* absolute configuration was assigned to the dextrorotatory enantiomers (+)-**4** and (+)-**5**.

The synthesis of the two enantiomers (*S*)-(−)-**7** and (*R*)-(+)-**7** is reported in Scheme 2. The imidazolines (*S*)-(+)-**13** and (*R*)-(−)-**13** were obtained by catalytic hydrogenation over Pd/C of the nitro-derivatives (*S*)-(−)-**3** and (*R*)-(+)-**3**.[11] Diazotization and subsequent hydrolysis of the corresponding arenediazonium salts yielded the imidazolines (*S*)-(−)-**7** and (*R*)-(+)-**7**. The enantiomeric purity of (*S*)-(−)-**7** and (*R*)-(+)-**7**, determined by ^{1}H NMR spectroscopy in comparison with the spectrum of racemic compound (±)-**7** and on addition of the chiral shift reagent (*R*)-(+)-α-methoxy-α-(trifluoromethyl)phenylacetic acid [(+)-(*R*)-MTPA], was found to be >98% (detection limit): the ^{1}H NMR spectrum of the racemic compound (±)-**7** showed a double doublet at δ 1.43 ppm for the methyl protons, whereas only one doublet was observed for (*S*)-(−)-**7** and (*R*)-(+)-**7** at δ 1.42 and 1.44 ppm, respectively.

Scheme 1[a]

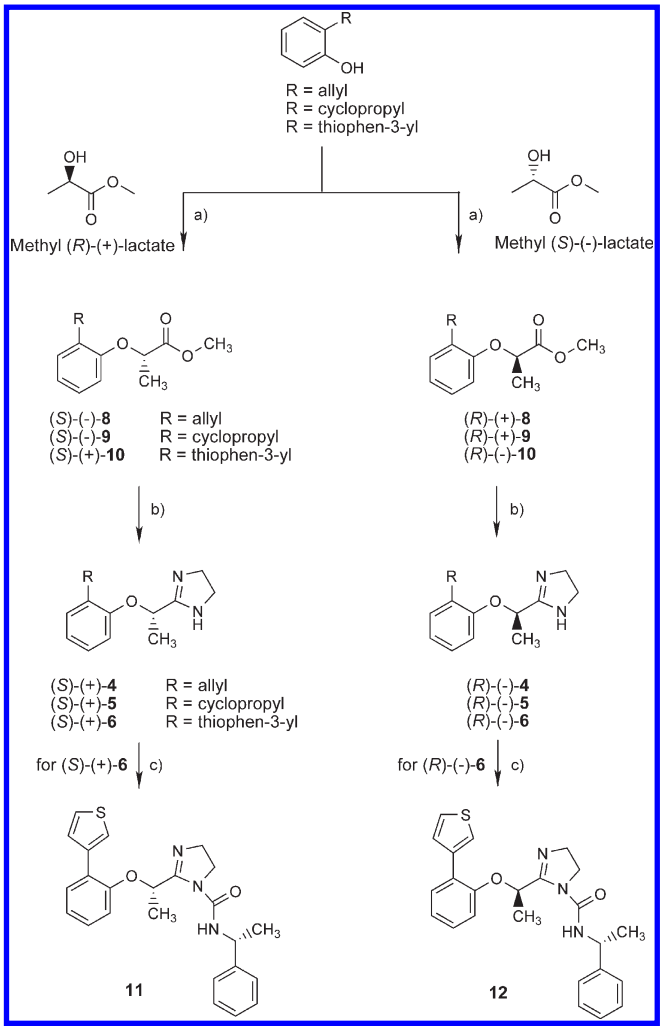

[a] Reagents: (a) DEAD, PPh_3, dry THF; (b) $(CH_3)_3Al$, NH_2CH_2-CH_2NH_2, dry toluene, Δ; (c) *R*-(+)-α-methylbenzyl isocyanate.

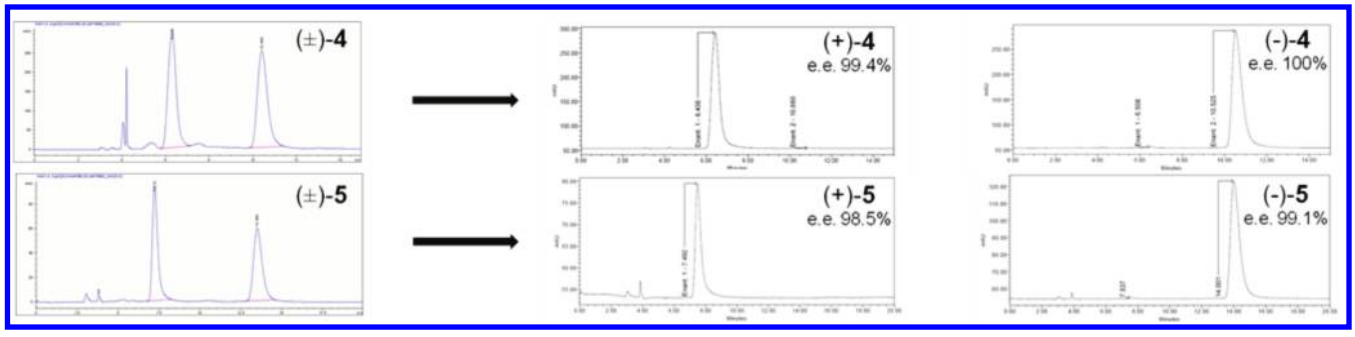

Figure 1. HPLC spectra of (±)-**4**, (±)-**5**, and their corresponding enantiomers.

Results and Discussion

The affinity values (pK_i), antagonist properties (pK_b), agonist potencies, and intrinsic activities (pEC_{50} and ia, respectively) of the novel compounds on α_2-AR subtypes are reported in Table 1. The biological profiles of the lead **1**, clonidine and imidazolines **2** and **3**, and their enantiomers were also included for useful comparison. Analogously to what was observed for the enantiomers of **2** and **3**,[11] both enantiomers of **4** and **5** displayed comparable binding affinity for a given α_2-AR subtype. Moreover, analogously to their corresponding racemic compounds,[6] they showed moderate α_{1a}-AR binding affinity ($pK_i \leq 6.5$) and negligible intrinsic activity (ia < 0.3). The functional results, demonstrating the role played by chirality, highlighted that for both pairs of the enantiomers, the (*S*) form behaved as eutomer and produced better α_{2C}-AR agonist activity; indeed, (*S*)-(+)-**4** and (*S*)-(+)-**5** fully activated this subtype with high potency (ia = 0.90; pEC_{50} = 7.60 and 7.45, respectively), while the corresponding distomers (*R*)-(−)-**4** and (*R*)-(−)-**5** behaved as partial agonists (Figure 2). The α_{2B}-AR subtype was moderately activated by (*S*)-(+)-**4** and (*S*)-(+)-**5** (ia = 0.65; pEC_{50} = 6.00 and 5.50, respectively); (*R*)-(−)-**4** and (*R*)-(−)-**5** were found to be inactive. Less affected by chirality, the significant α_{2A}-AR antagonism of **4** and **5** was maintained by (*R*)-(−)-**4** and (*R*)-(−)-**5** and moderately enhanced by (*S*)-(+)-**4** and (*S*)-(+)-**5** (Figure 3). We previously reported[11] the surprising reversal of enantioselectivity observed for the structurally similar compounds **2** and **3**, whose (*S*) and (*R*) forms, respectively, were the preferred α_{2C}-AR configurations. The higher α_{2C}-potencies displayed by (*S*)-(+)-**4** and (*S*)-(+)-**5** confirmed our previous results according to which the interactions between the aromatic cluster of the α_2-AR binding cavity and the ortho pendant moiety depended on the physicochemical characteristics of this latter.[8] Indeed, the pendant phenyl, allyl, and cyclopropyl substituents of (*S*)-(−)-**2**, (*S*)-(+)-**4**, and (*S*)-(+)-**5**, respectively, endowed with the same $+\pi$ and $-\sigma$ character and spatial orientation, and presumably, recognizing common amino acidic residues, gave more efficient lipophilic interactions. On the contrary, in the case of **3**, the polar interaction determined by the meta nitro group ($-\pi$ and $+\sigma$), was more favorably obtained by the inverse configuration. Further support for this hypothesized pathway has been provided by the examination of the functional behavior of the enantiomeric pairs of **6** and **7**, prepared in this study (Table 1). The α_{2C}-AR preferred configurations [(*S*)-(+)-**6** (pEC_{50} = 8.2; ia = 0.90) or (*R*)-(+)-**7** (pEC_{50} = 7.60; ia = 1.0)] were expected, because, in agreement with the peculiar nature of the thiophen-3-yl or *meta*-hydroxy phenyl pendant moieties, characterized by $+\pi$ and $-\sigma$ or $-\pi$ and $+\sigma$ conditions, respectively. On the other hand, it has already been reported that modifications on ligands belonging to the same series can produce changes in their binding mode.[15] Moreover, the enantiomers of **6** and **7** displayed α_{2A}- and α_{2B}-AR profiles similar to those of the corresponding enantiomers of the parents **2** or **3**, respectively. Anyway, the ability of the stereocenter in the bridge in affecting significantly the α_2-AR agonism or negligibly the α_2-AR antagonism is observed for all compounds of this series.

The data from the in vivo studies showed that, surprisingly, the pretreatment with (*S*)-(+)-**4** or (*R*)-(−)-**4** enhanced to the same extent morphine analgesia with an effect comparable to that of the racemic compound **4**.[6] This effect was rapid (30 min), potent, and long lasting (duration 240 min). Analogous behavior was observed for the (*S*)-(+)-**5** and (*R*)-(−)-**5** pair (Figure 4A,B). The α_{2C}-AR potencies shown by the distomers

Scheme 2[a]

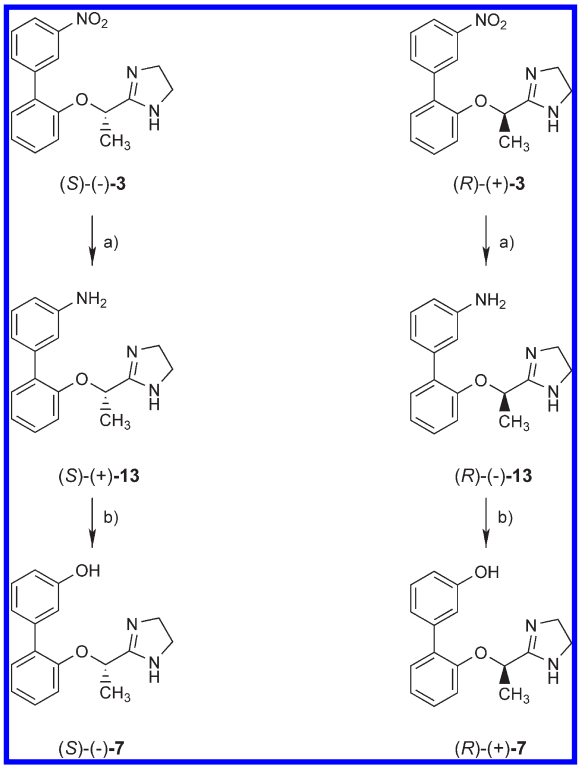

[a] Reagents: (a) H_2/Pd, (b) H_2SO_4, H_2O, $NaNO_2$; H_2O, $Cu(NO_3)_2 \cdot 3H_2O$, Cu_2O.

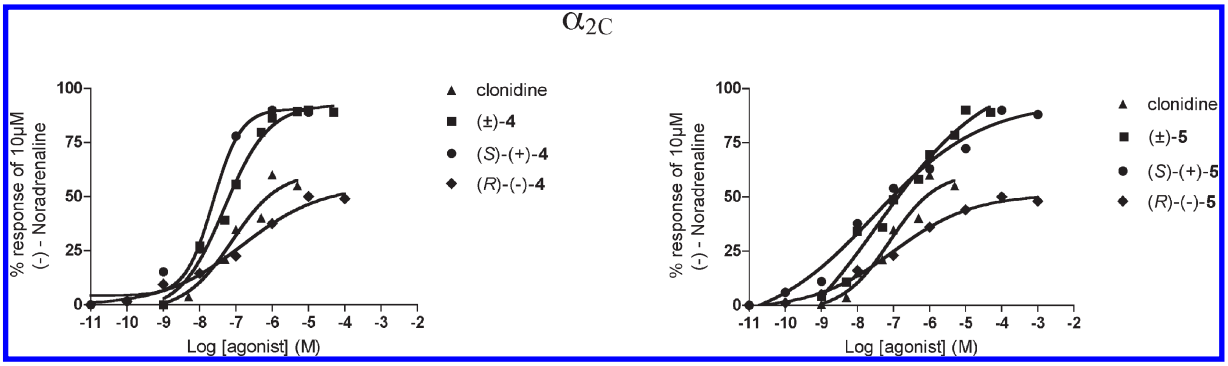

Figure 2. Agonist potencies of clonidine, (±)-**4**, (±)-**5**, and their corresponding enantiomers determined by Cytosensor microphysiometer in CHO cells stably expressing the human α_{2C}-AR subtype.

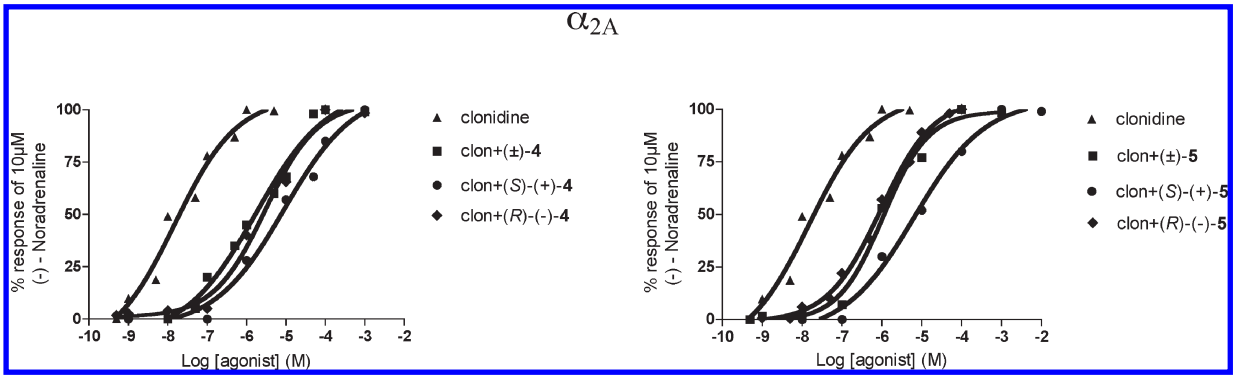

Figure 3. Antagonist potencies of (±)-**4**, (±)-**5**, and their corresponding enantiomers determined by Cytosensor microphysiometer in CHO cells stably expressing the human α_{2A}-AR subtype.

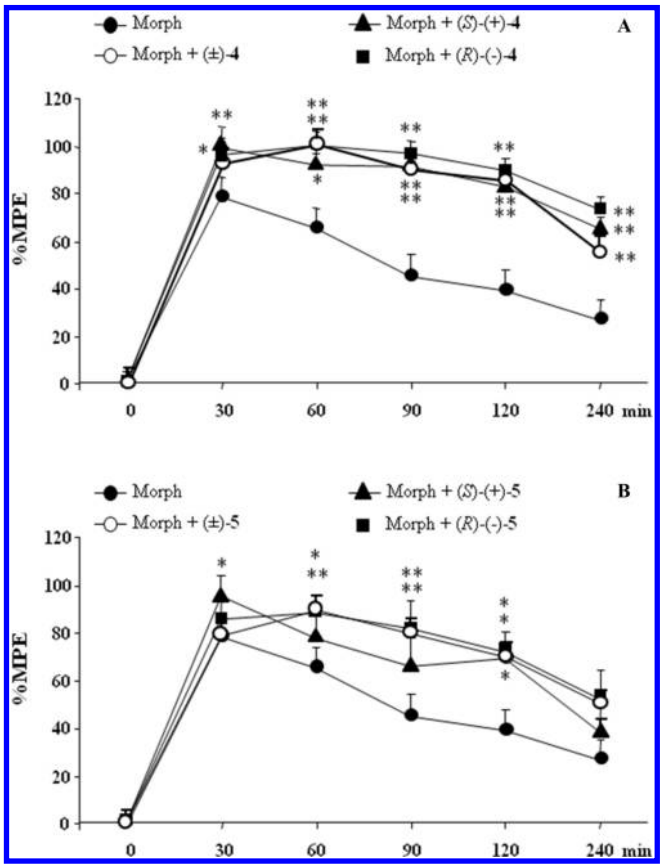

Figure 4. Effect of a single administration of (±)-**4** (A) or (±)-**5** (B) and their corresponding enantiomers on morphine-induced analgesia in the tail-flick test. The reaction latencies were expressed as a percent of the maximum possible effect (%MPE). Each point represents the media ± SEM of eight animals. Significant differences: *$p < 0.05$, **$p < 0.01$ compared to morphine group.

(*R*)-(−)-**4** and (*R*)-(−)-**5** (ia = 0.50; pEC_{50} = 6.73 and 6.90, respectively), comparable to that of clonidine (pEC_{50} α_{2C} = 7.24; ia = 0.60), may explain their significant morphine analgesia enhancement. As with the corresponding racemic compounds, the novel derivatives had no analgesic effect when given alone (data not shown). The fact that pretreatment with the α_2-AR antagonist yohimbine blocked the effects of both (*S*)-(+)-**4** and (*R*)-(−)-**4** unambiguously demonstrated the involvement of the α_{2C}-AR activation in the positive morphine analgesia modulation of both enantiomers (Figure 5). Surprisingly, a full α_{2C}-AR activation appeared advantageous to contrast the expression of morphine tolerance. Indeed, while

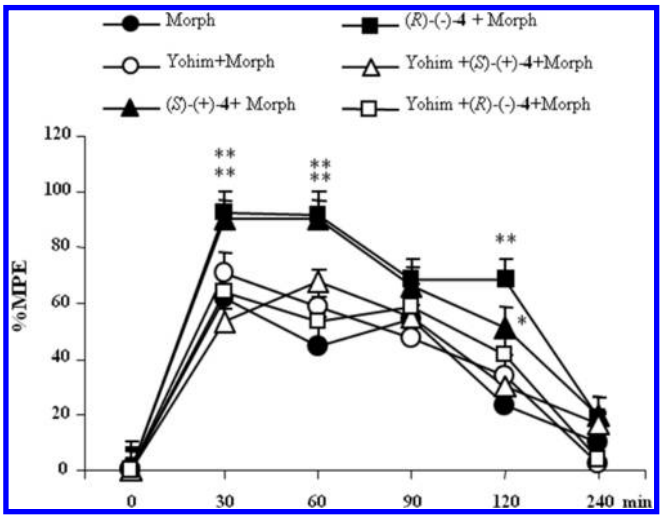

Figure 5. Effect of (*S*)-(+)-**4** and (*R*)-(−)-**4** on morphine-induced analgesia after yohimbine pretreatment in the tail-flick test. The reaction latencies were expressed as a percent of the maximum possible effect (% MPE). Each point represents the media ± SEM of 7−8 animals. Significant differences: *$p < 0.05$, **$p < 0.01$ compared to morphine group.

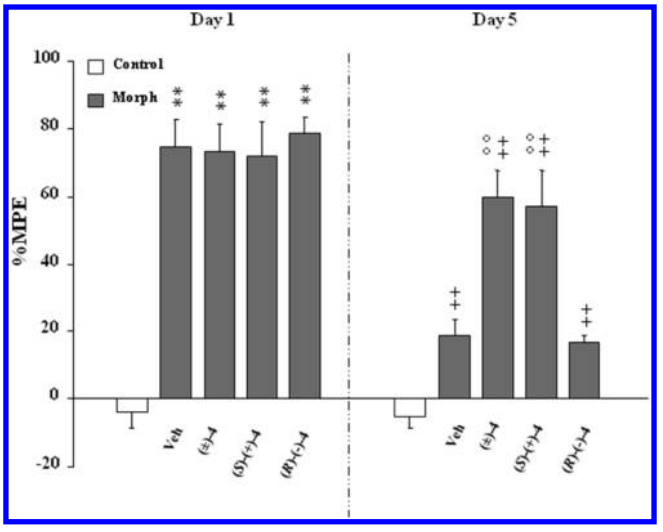

Figure 6. Effect of a single administration of (±)-**4**, (*S*)-(+)-**4**, and (*R*)-(−)-**4** on expression of tolerance to morphine-induced analgesia. Antinociceptive effect (% MPE) on control (n = 10) or morphine (n = 36) treated mice was evaluated on day 1 and day 5. Significant differences: **$p < 0.01$, compared to control group; ++$p < 0.01$, compared to related-morphine group on day 1; °°$p < 0.01$, compared to morphine group on day 5.

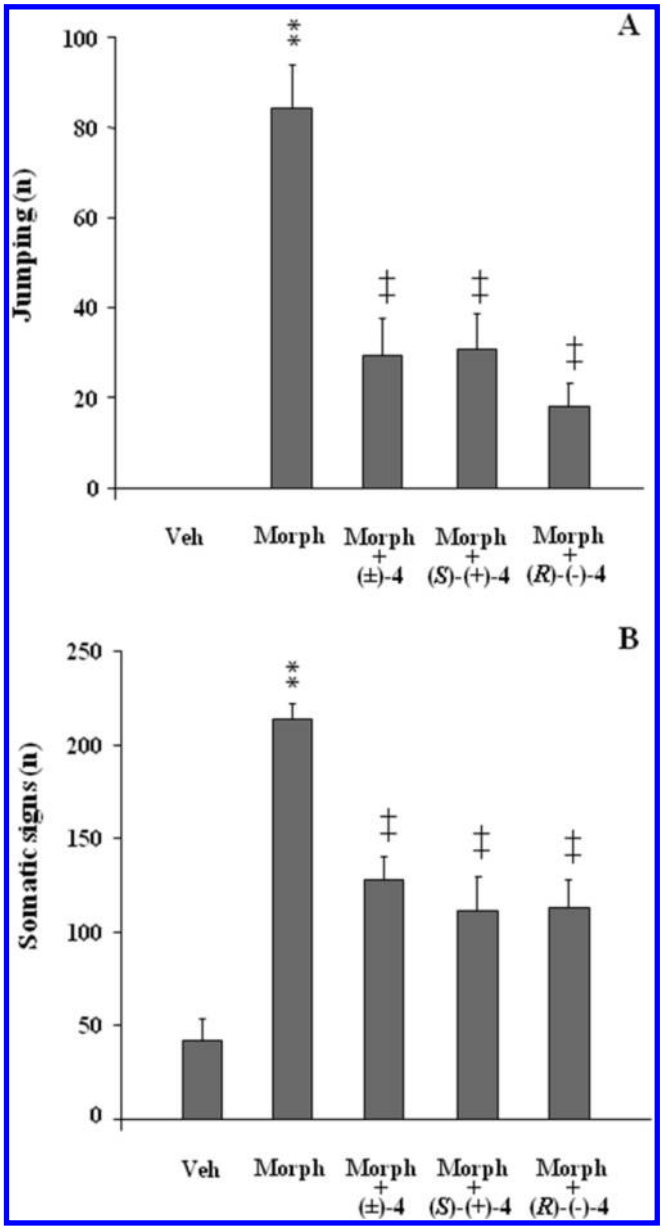

Figure 7. Effect of a single administration of (±)-**4**, (*S*)-(+)-**4**, and (*R*)-(−)-**4** on the expression of morphine dependence. Naloxone-precipitated withdrawal symptoms, both in control (n = 10) and morphine (n = 36) treated mice, are given as a measure of the frequency of jumping (A) and somatic signs (B) expressed as summary of rearing, forepaw tremors, and teeth chatter. Significant differences: **$p < 0.01$, compared to vehicle; ++$p < 0.01$, compared to morphine group.

(*R*)-(−)-**4** was ineffective, the acute administration of a 0.05 mg/kg dose of **4** or its enantiomer (*S*)-(+)-**4**, 15 min before the last morphine treatment on the test day, reduced the analgesic effect only of 22% compared to 74% observed for alone morphine-treated group (Figure 6). The acute administration of **4** or its enantiomers, 15 min before naloxone injection, significantly decreased the expression of naloxone-precipitated withdrawal syndrome: the frequencies of jumping and other somatic signs, such as rearing, paw tremor, and teeth chatter, were halved (Figure 7A,B). Clonidine also appears to attenuate the expression of morphine tolerance and withdrawal symptoms, but at higher doses (2 and 5 mg/kg for tolerance and dependence expression, respectively) and with associated sedation and hypotension side effects.[16] Instead, **4**, (*S*)-(+)-**4**, and (*R*)-(−)-**4**

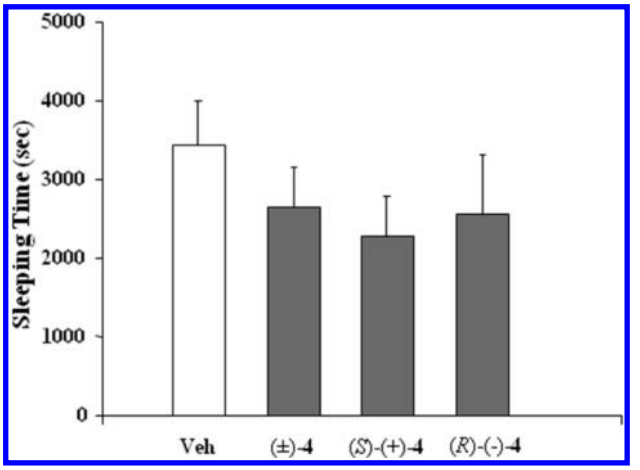

Figure 8. Effect of (±)-**4**, (*S*)-(+)-**4**, and (*R*)-(−)-**4** on pentobarbital sodium-induced sleep time. Mice were treated with 50 mg/kg pentobarbital sodium (Pent; n = 40) 15 min after the administration of 0.05 mg/kg (±)-4 and its enantiomers. The sleeping time was expressed in seconds. No significant differences were observed.

were devoid of sedative effects (Figure 8). Moreover, unlike clonidine,[16,17] the repeated treatment with **4** or its enantiomers, before each morphine administration, decreased acquisition of tolerance and dependence. Significant enhancement of the morphine analgesia both on day 1 and on day 5 was observed (Figure 9); in addition, the naloxone-induced behavioral withdrawal symptoms proved reduced. Total signs were decreased by about 40%, while jumping was almost completely blocked by **4**; in this case, the observed reduction was 80% (Figure 10A,B). The positive effects on dependence are important because withdrawal symptoms are believed to have a major role in relapse to drug-taking behavior after detoxification.[18]

Conclusion

In summary, the study of **4** and its enantiomers, confirming the involvement of the α_{2C}-AR in morphine analgesia,[5,6] suggests that the partial activation of this subtype proved to be compatible with (i) sharp enhancement of morphine analgesia and (ii) effective reduction of acquisition of morphine tolerance as well as acquisition and expression of morphine dependence. The distomer (*R*)-(−)-**4** displayed these effects similarly to the full agonists **4** and (*S*)-(+)-**4**. On the other hand, the full α_{2C}-AR activation, as that triggered by **4** and (*S*)-(+)-**4**, appeared advantageous in reducing the expression of morphine tolerance. Therefore, **4** and (*S*)-(+)-**4**, enhancing morphine analgesia and decreasing both acquisition and expression of morphine tolerance and dependence, displayed an unusual biological profile and could become novel promising therapeutic tools in the management of chronic pain and opioid addiction. In addition, the assessment of the physicochemical and in vitro ADME properties of **4** showed it to be highly soluble in water at physiological pH and have a high level of metabolic stability in both mouse and human microsomal preparations. It also exhibits high passive diffusion in an artificial phospholipid membrane (PAMPA)[19] and an MDCK cell line, with no issues of P-glycoprotein (PGP)-mediated efflux. Although an in vivo PK and brain−plasma distribution was not carried out, the in vitro profile of this compound bodes well for significant brain exposure and is in line with the observed central effects in the pharmacology models.

Finally, considering that (i) clonidine is ineffective to prevent the development of morphine tolerance,[16,17] but is clinically

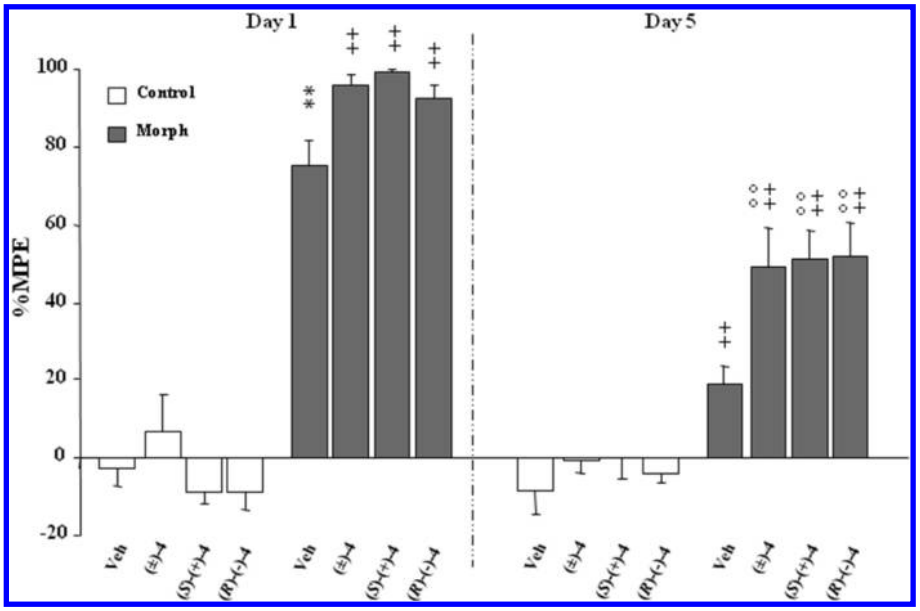

Figure 9. Effect of repeated administration of (±)-**4**, (*S*)-(+)-**4**, and (*R*)-(−)-**4** on the acquisition of tolerance to morphine-induced analgesia. Antinociceptive effect (% MPE) on control (n = 30) or morphine (n = 41) treated mice was evaluated on day 1 and day 5. Significant differences: $^{**}p < 0.01$, compared to control group; $^{++}p < 0.01$, compared to related-morphine group on day 1; $^{\circ\circ}p < 0.01$, compared to morphine group on day 5.

effective at reducing the intensity of withdrawal symptoms, increasing treatment duration and completion,[20,21] (ii) morphine withdrawal-induced jumping was attenuated in α_{2A}-AR KO mice,[17] and (iii) the chronic application of yohimbine attenuated naloxone-induced opioid withdrawal in mice[22] and partially prevented opioid withdrawal signs in methadone maintained patients,[23] we might attribute the unique profiles of **4** (named allyphenyline) and (*S*)-(+)-**4** to the synergistic combination of their potent α_{2C}-AR agonism/α_{2A}-AR antagonism.

Experimental Protocols

Chemistry. Melting points were taken in glass capillary tubes on a Buchi SMP-20 apparatus and are uncorrected. IR and NMR spectra were recorded on Perkin-Elmer 297 and Varian EM-390 instruments, respectively. Chemical shifts are reported in parts per million (ppm) relative to tetramethylsilane (TMS), and spin multiplicities are given as s (singlet), d (doublet), t (triplet), q (quartet), or m (multiplet). IR spectral data (not shown because of the lack of unusual features) were obtained for all compounds reported and are consistent with the assigned structures. The microanalyses were performed by the Microanalytical Laboratory of the department of Chemical Sciences of the University of Camerino. The elemental composition of the compounds agreed to within ±0.4% of the calculated value. Optical rotation was measured at a 1 g/100 mL concentration (c = 1) with a Perkin-Elmer 241 polarimeter (accuracy ±0.002°). Chromatographic separations were performed on silica gel columns (Kieselgel 40, 0.040−0.063 mm, Merck) by flash chromatography. Compounds were named following IUPAC rules as applied by ChemBioDraw Ultra (version 11.0) software for systematically naming organic chemicals. HPLC analyses of (*S*)-(+)-**6** and (*R*)-(−)-**6** were recorded on an Hewelett Packard 1090 I series chromatograph on a Hypersil 200 mm × 2.1 mm stainless steel column (packed with 5 μm particles, Hewlett-Packard). The mobile phase used was hexane/AcOEt (60/40), and the flow rate was set at 1.0 mL/min. The purity of the new compounds was determined by combustion analysis and was ≥95%.

Enantiomeric Separation of Racemic Compounds (±)-4 and (±)-5. The enantiomers of the title compounds[6] were separated by chiral HPLC by using a chiral column Chiralcel OD-H (25 cm × 0.46 cm, 5 μm particle size), mobile phase: *n*-hexane/2-propanol 90/10 v/v for (±)-**4** or *n*-hexane/2-propanol 85/15 v/v for (±)-**5**; flow rate 1 mL/min; detection was monitored at a wavelength of 220 nM: run time 15.0 min for compound (±)-**4** and 18.0 min for compound (±)-**5** (Figure 1). Retention times: (+)-**4** 6.51 min; (−)-**4** 10.52 min; (+)-**5** 7.54 min; (−)-**5** 14.00 min; ee ≥ 99%.

The free bases were transformed into the hydrogen oxalate salts, which were recrystallized from EtOH:

(+)-**4**: $[\alpha]^{20}_D$ = +2.56° (*c* 1, MeOH); mp 154−155 °C. ^{1}H NMR (DMSO) δ 1.53 (d, 3, CHC*H*$_3$), 3.42 (m, 2, C*H*$_2$CH), 3.88 (s, 4, NC*H*$_2$C*H*$_2$N), 5.06 (dd, 2, CH=C*H*$_2$), 5.40 (q, 1, OC*H*), 5.95 (m, 1, C*H*=CH$_2$), 6.92−7.26 (m, 4, Ar*H*), 7.81 (br s, 1, NH, exchangeable with D$_2$O). Anal. (C$_{14}$H$_{18}$N$_2$O·H$_2$C$_2$O$_4$) C, H, N.

(−)-**4**: $[\alpha]^{20}_D$ = −2.67° (*c* 1, MeOH); mp 154−155 °C. ^{1}H NMR (DMSO) δ 1.53 (d, 3, CHC*H*$_3$), 3.42 (m, 2, C*H*$_2$CH), 3.88 (s, 4, NC*H*$_2$C*H*$_2$N), 5.06 (dd, 2, CH=C*H*$_2$), 5.40 (q, 1, OC*H*), 5.95 (m, 1, C*H*=CH$_2$), 6.92−7.26 (m, 4, Ar*H*), 7.81 (br s, 1, NH, exchangeable with D$_2$O). Anal. (C$_{14}$H$_{18}$N$_2$O·H$_2$C$_2$O$_4$) C, H, N.

(+)-**5**: $[\alpha]^{20}_D$ = +0.68° (*c* 1, MeOH); mp 141−142 °C. ^{1}H NMR (DMSO) δ 0.51−0.98 (m, 4, *CH*$_2$*CH*$_2$), 2.58 (d, 3, CHC*H*$_3$), 2.24 (m, 1, C*H*), 3.91 (s, 4, NC*H*$_2$C*H*$_2$N), 5.37 (q, 1, OC*H*), 6.83−7.18 (m, 4, Ar*H*), 9.51 (br s, 1, N*H*, exchangeable with D$_2$O). Anal. (C$_{14}$H$_{18}$N$_2$O·H$_2$C$_2$O$_4$) C, H, N.

(−)-**5**: $[\alpha]^{20}_D$ = −0.63° (*c* 1, MeOH); mp 141−142 °C. ^{1}H NMR (DMSO) δ 0.51−0.98 (m, 4, *CH*$_2$*CH*$_2$), 2.58 (d, 3, CHC*H*$_3$), 2.24 (m, 1, C*H*), 3.91 (s, 4, NC*H*$_2$C*H*$_2$N), 5.37 (q, 1, OC*H*), 6.83−7.18 (m, 4, Ar*H*), 9.51 (br s, 1, N*H*, exchangeable with D$_2$O). Anal. (C$_{14}$H$_{18}$N$_2$O·H$_2$C$_2$O$_4$) C, H, N.

(*S*)-(−)-Methyl 2-(2-allylphenoxy)propanoate [(*S*)-(−)-8]. A solution of DEAD (3.01 g, 14.9 mmol) in dry THF (10 mL) was added dropwise to a mixture of methyl (*R*)-(+)-lactate (1.36 g, 13.1 mmol), 2-allylphenol (1.70 g, 12.7 mmol), and triphenylphosphine (3.34 g, 12.7 mmol) in THF (20 mL). The mixture was stirred at room temperature under nitrogen atmosphere overnight. The solvent was evaporated, and diethyl ether/hexane solution was added. The precipitate triphenylphosphine oxide was filtered off, and the removal of the dried solvent gave a residue that was purified by flash chromatography eluting with cyclohexane/AcOEt (95:5) (2.37 g,

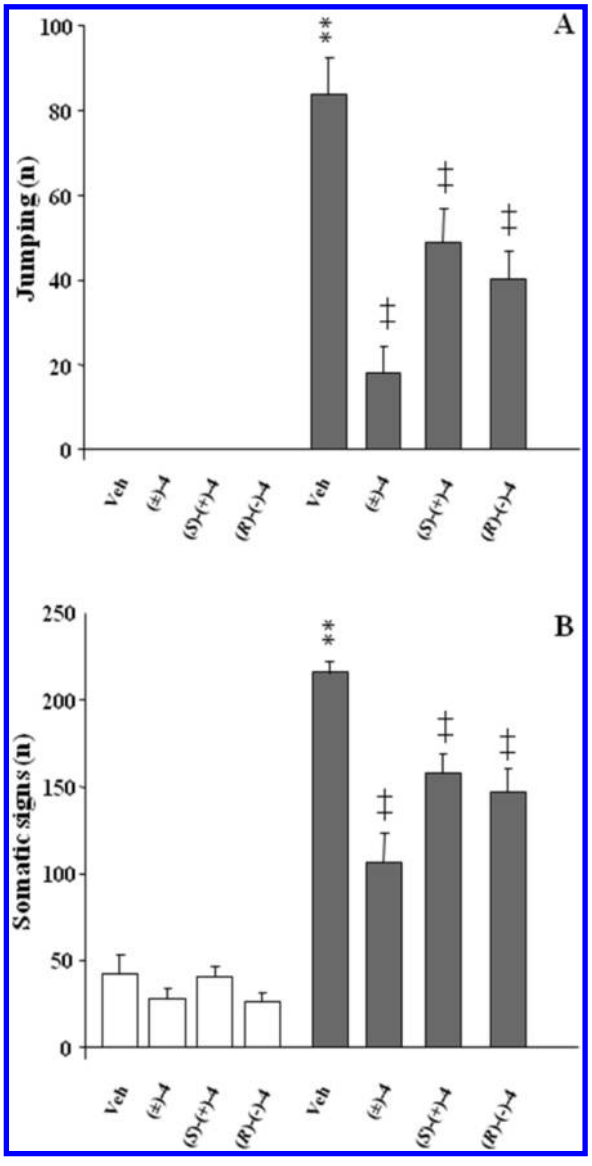

Figure 10. Effect of repeated administration of (±)-**4**, (*S*)-(+)-**4**, and (*R*)-(−)-**4** on the acquisition of morphine dependence. Naloxone-precipitated withdrawal symptoms, both in control (n = 30) and morphine (n = 41) treated mice, are given as a measure of the frequency of jumping (A) and somatic signs (B) expressed as summary of rearing, forepaw tremors, and teeth chatter. Significant differences: **p < 0.01, compared to vehicle; ++p < 0.01, compared to morphine group.

85% yield): $[\alpha]^{20}_D$ = −7.18° (*c* 1, $CHCl_3$). ^{1}H NMR ($CDCl_3$) δ 1.61 (d, 3, $CHCH_3$), 3.44 (m, 2, CH_2CH), 3.76 (s, 3, OCH_3) 4.78 (q, 1, OC*H*), 5.08 (dd, 2, $CH{=}CH_2$), 6.01 (m, 1, $CH{=}CH_2$), 6.71−7.19 (m, 4, Ar*H*).

(*R*)-(+)-Methyl 2-(2-allylphenoxy)propanoate [(*R*)-(+)-8]. This was prepared as described for (*S*)-(−)-**8** starting from methyl (*S*)-(−)-lactate (81% yield): $[\alpha]^{20}_D$ = +7.33° (*c* 1, $CHCl_3$). ^{1}H NMR ($CDCl_3$) δ 1.61 (d, 3, $CHCH_3$), 3.44 (m, 2, CH_2CH), 3.76 (s, 3, OCH_3) 4.78 (q, 1, OC*H*), 5.08 (dd, 2, $CH{=}CH_2$), 6.01 (m, 1, $CH{=}CH_2$), 6.71−7.19 (m, 4, Ar*H*).

(*S*)-(+)-2-(1-(2-Allylphenoxy)ethyl)-4,5-dihydro-1*H*-imidazole [(*S*)-(+)-4]. A solution of ethylenediamine (0.42 mL, 6.28 mmol) in dry toluene (4 mL) was added dropwise to a mechanically stirred solution of 2 M trimethylaluminum (3.2 mL, 6.28 mmol) in dry toluene (4 mL) at 0 °C under nitrogen atmosphere. After 1 h, the solution was cooled to 0 °C, and a solution of (*S*)-(−)-**8** (0.69 g, 3.14 mmol) in dry toluene (8 mL) was added dropwise. The mixture was heated to 65 °C for 3 h, cooled to 0 °C, and quenched cautiously with MeOH (0.8 mL), followed by H_2O (0.2 mL). After addition of $CHCl_3$ (5 mL) and filtration, the organic layer was extracted with 2 N HCl. The aqueous layer, made basic with 10% NaOH, was extracted with $CHCl_3$. Removal of dried solvent gave the free base (*S*)-(+)-**4**, which was purified by flash chromatography using cyclohexane/AcOEt/MeOH/33% NH_4OH (6:3:1:0.1) (63% yield). The enantiomeric purity, determined by HPLC by using a chiral column Chiralcel OD-H (25 cm × 0.46 cm), eluent *n*-hexane/2-propanol 90/10 v/v, was about 85%. $[\alpha]^{20}_D$ = +1.75° (*c* 1, MeOH). ^{1}H NMR (DMSO) δ 1.53 (d, 3, $CHCH_3$), 3.42 (m, 2, CH_2CH), 3.88 (s, 4, NCH_2CH_2N), 5.06 (dd, 2, $CH{=}CH_2$), 5.40 (q, 1, OC*H*), 5.95 (m, 1, $CH{=}CH_2$), 6.92−7.26 (m, 4, Ar*H*), 7.81 (br s, 1, NH, exchangeable with D_2O).

(*R*)-(−)-2-(1-(2-Allylphenoxy)ethyl)-4,5-dihydro-1*H*-imidazole [(*R*)-(−)-4]. This was prepared as described for (*S*)-(+)-**4** starting from (*R*)-(+)-**8** (59% yield). The enantiomeric purity, determined by HPLC by using a chiral column Chiralcel OD-H (25 cm × 0.46 cm), eluent *n*-hexane/2-propanol 90/10 v/v, was about 85%. $[\alpha]^{20}_D$ = −1.64° (*c* 1, MeOH). ^{1}H NMR (DMSO) δ 1.53 (d, 3, $CHCH_3$), 3.42 (m, 2, CH_2CH), 3.88 (s, 4, NCH_2CH_2N), 5.06 (dd, 2, $CH{=}CH_2$), 5.40 (q, 1, OC*H*), 5.95 (m, 1, $CH{=}CH_2$), 6.92−7.26 (m, 4, Ar*H*), 7.81 (br s, 1, NH, exchangeable with D_2O).

***N*-((*R*)-1-Phenylethyl)-2-((*S*)-1-(2-(thiophen-3-yl)phenoxy)ethyl)-4,5-dihydro-1*H*-imidazole-1-carboxamide (11).** (*R*)-(+)-α-Methylbenzyl isocyanate (0.14 g, 0.95 mmol) was added to a solution of (*S*)-(+)-**6** (0.26 g, 0.95 mmol) in dry CH_2Cl_2. After 4 h at room temperature, the solvent was removed and the residue was purified by flash chromatography using cyclohexane/AcOEt (5:5). ^{1}H NMR ($CDCl_3$) δ 1.40 (d, 3, $OCHCH_3$), 1.60 (d, 3, CH_3CHN), 3.82 (m, 4, NCH_2CH_2N), 5.05 (m, 1, C*H*N), 5.50 (d, 1, N*H*, exchangeable with D_2O), 5.85 (q, 1, OC*H*), 6.90−8.75 (m, 12, Ar*H*).

***N*-((*R*)-1-Phenylethyl)-2-((*R*)-1-(2-(thiophen-3-yl)phenoxy)ethyl)-4,5-dihydro-1*H*-imidazole-1-carboxamide (12).** This was prepared as described for **11** starting from (*R*)-(−)-**6** (53% yield). ^{1}H NMR ($CDCl_3$) δ 1.39 (d, 3, $OCHCH_3$), 1.70 (d, 3, CH_3CHN), 3.82 (m, 4, NCH_2CH_2N), 5.01 (m, 1, C*H*N), 5.50 (d, 1, N*H*, exchangeable with D_2O), 5.80 (q, 1, OC*H*), 6.90−8.75 (m, 12, Ar*H*).

(*S*)-(+)-2′-(1-(4,5-Dihydro-1*H*-imidazol-2-yl)ethoxy)biphenyl-3-amine Hydrogen Oxalate Salt [(*S*)-(+)-13]. A solution of (*S*)-(−)-**3**[11] (1.0 g, 3.2 mmol) in MeOH (20 mL) was hydrogenated for 8 h at room temperature under pressure (40 psi) using Pd/C as catalyst. After catalyst removal, the evaporation of the solvent gave the free base which was purified by flash chromatography. Eluting with cyclohexane/AcOEt/MeOH/33% NH_4OH (5:4:1:0.1) afforded the free base (0.27 g, 30% yield), which was transformed into the hydrogen oxalate salt; recrystallized from EtOH: $[\alpha]^{20}_D$ = +6.76° (*c* 1, MeOH); mp 158.8−160.5 °C. ^{1}H NMR (DMSO) δ 1.50 (d, 3, $CHCH_3$), 3.82 (s, 4, NCH_2CH_2N), 5.10 (q, 1, OC*H*), 6.50−7.40 (m, 8, Ar*H*), 8.92 (br s, 2, NH_2 exchangeable with D_2O)10.5 (br s, 1, N*H*, exchangeable with D_2O).

(*R*)-(−)-2′-(1-(4,5-Dihydro-1*H*-imidazol-2-yl)ethoxy)biphenyl-3-amine Hydrogen Oxalate Salt [(*R*)-(−)-13]. This was prepared as described for (*S*)-(+)-**13** starting from (*R*)-(+)-**3**[11] (39% yield). The free base was transformed into the hydrogen oxalate salt, which was recrystallized from EtOH: $[\alpha]^{20}_D$ = −6.25° (*c* 1, MeOH); mp 155.6−157.4 °C. ^{1}H NMR (DMSO) δ 1.50 (d, 3, $CHCH_3$), 3.82 (s, 4, NCH_2CH_2N), 5.10 (q, 1, OC*H*), 6.50−7.40 (m, 8, Ar*H*), 8.92 (br s, 2, NH_2 exchangeable with D_2O), 10.5 (br s, 1, N*H*, exchangeable with D_2O).

(*S*)-(−)-2′-[1-(4,5-Dihydro-1*H*-imidazol-2-yl)-ethoxy]-biphenyl-3-ol Hydrochloride Salt [(*S*)-(−)-7]. Crushed ice was added to a solution of (*S*)-(+)-**13** (0.3 g, 1.07 mmol) in 26% sulfuric acid (24 mL). The stirred mixture was maintained at 0−5 °C, and a solution of sodium nitrite (0.07 g, 1.01 mmol) in water (0.86 mL) was slowly added. After the addition, the mixture was left at the same temperature for 15 min. Urea was added to remove the excess of sodium nitrite. A solution of copper(II) nitrate trihydrate (2.54 g, 10.5 mmol) in water (20.4 mL) was added to the freshly

prepared solution of diazonium salt maintained at 0 °C, then copper(I) oxide (0.12 g, 0.84 mmol) was added to the vigorously stirred mixture, and gas evolution being observed. The reaction mixture was left at room temperature for 30 min, then basified with $NaHCO_3$ and extracted with dichloromethane. Removal of dried solvent gave the free base (*S*)-(−)-**7**, which was purified by flash chromatography using cyclohexane/AcOEt/MeOH/33% NH_4OH (6:4:1.5:0.1): (0.1 g, 33% yield). The free base was transformed into the hydrochloride salt (oil). $[\alpha]^{20}_D = -2.30°$ (*c* 1, MeOH). ^{1}H NMR (DMSO) δ 1.40 (d, 3, $CHCH_3$), 3.80 (s, 4, NCH_2CH_2N), 4.95 (q, 1, OC*H*), 6.70−7.38 (m, 8, Ar*H*), 7.68 (br s, 1, O*H*, exchangeable with D_2O), 10.17 (br s, 1, N*H*, exchangeable with D_2O). Anal. ($C_{17}H_{18}N_2O_2 \cdot HCl$) C, H, N.

(*R*)-(+)-2′-[1-(4,5-Dihydro-1*H*-imidazol-2-yl)-ethoxy]-biphenyl-3-ol Hydrochloride Salt [(*R*)-(+)-7]. This was prepared as described for (*S*)-(−)-**7** starting from (*R*)-(−)-1**3** (39% yield). The free base was transformed into the hydrochloride salt (oil). $[\alpha]^{20}_D = +2.15°$ (*c* 1, MeOH). ^{1}H NMR (DMSO) δ 1.40 (d, 3, $CHCH_3$), 3.80 (s, 4, NCH_2CH_2N), 4.95 (q, 1, OC*H*), 6.70−7.38 (m, 8, Ar*H*), 7.68 (br s, 1, O*H*, exchangeable with D_2O), 10.17 (br s, 1, N*H*, exchangeable with D_2O). ($C_{17}H_{18}N_2O_2 \cdot HCl$) C, H, N.

Biological Experiments. Culture of CHO Clones Expressing α_2-AR Subtypes. The plasmids used to stably express the human α_{2A}-, α_{2B}-, or α_{2C}-AR in CHO cells have been previously described.[24] Briefly, each vector contains an expression cassette comprising the CMV promoter/enhancer, the coding region of α_2C10-, α_2C2-, or α_2C4-gene, the IRES derived from the encephalomyocarditis virus, the neomycin phosphotransferase gene, and a fragment from the rabbit β-globin gene containing an intron and a polyadenylation signal. Cells were transfected using the calcium phosphate method, and clones were selected in the presence of G418-sulfate (1 mg/mL). CHO-α_{2A}, CHO-α_{2B}, and CHO-α_{2C} were routinely subcultured in Dulbecco's Modified Eagle's Medium (DMEM) supplemented with 10% fetal calf serum. The clones used in this study respectively express 1.45 ± 0.3, 4.2 ± 0.8, and 2.7 ± 0.5 pmol of receptor/mg of membrane protein.

Binding Experiments. Binding studies were performed on crude cell membrane preparations using the selective α_2-antagonist, [^{3}H]RX 821002, as radioligand. Briefly, membranes were incubated in a final volume of 400 μL of Tris-Mg buffer (50 mM Tris-HCl, 0.5 mM $MgCl_2$, pH 7.5) containing the radioligand at a concentration corresponding to twice its K_d value for the considered subtype (3 nM for CHO-α_{2A}, 10 nM for CHO-α_{2B}, and 6 nM for CHO-α_{2C}) and increasing concentrations (10^{-9} to 10^{-4} M) of the competitor to be tested. After 30 min of incubation at room temperature, membrane bound radioactivity was collected by filtration through a fiberglass filter (Whatman GFC) using a Skatron cell harvester. Filters were rapidly washed, transferred to scintillation vials, and counted for radioactivity. Inhibition data were analyzed using the GraphPad Prism computer program (GraphPad Software Inc., San Diego, CA, USA), allowing nonlinear regression analysis according to a one- or a two-site inhibition model.

Binding to cloned human α_1-AR subtypes was performed in membranes from CHO cells transfected by electroporation with DNA expressing the gene encoding each α_1-AR subtype. Cloning and stable expression of the human α_1-AR gene were performed as described in ref 25. CHO cell membranes (30 μg proteins) were incubated in 50 mM Tris-HCl, pH 7.4, with 0.1−0.4 nM [^{3}H]prazosin, in a final volume of 1.02 mL for 30 min at 25 °C, in the absence or presence of competing drugs (1 pM to 10 μM). Nonspecific binding was determined in the presence of 10 μM phentolamine. The incubation was stopped by addition of ice-cold Tris-HCl buffer and rapid filtration through 0.2% polyethyleneimine pretreated Whatman GF/B or Schleicher & Schuell GF52 filters.

Functional Assays: Cytosensor Microphysiometry. Extracellular acidification was measured using an eight-channel Cytosensor microphysiometry instrument (Molecular Devices, Menlo Park, CA, USA). CHO cells expressing individually human α_2-AR subtypes or α_{1A}-AR were seeded into 12 mm capsule cups at a density of 3×10^5 cells/cup and incubated at 37 °C under 5% CO_2 atmosphere for 24 h. The capsule cups were loaded into the sensor chambers of the instrument and perfused with a running medium (bicarbonate-free DMEM containing 0.584 g/L glutamine and 2.59 g/L NaCl) at a flow rate of 100 μL/min. Agonists were diluted into running medium and injected through a second fluid path. Valves directed the flow from either fluid path to the sensor chamber. For each 90 s pump cycle, the pump was on for 60 s and was then switched off for the remaining 30 s and the pH value was recorded for 20 s (from second 68−88). Cells were exposed to agonists for 4 min, and consecutive agonist exposures were separated by a 30 min washing period. This stimulation protocol was validated in preliminary experiments with four known agonists, (−)-noradrenaline, clonidine, UK 14304, and BHT 920 for α_2-AR CHO cells and (−)-noradrenaline and cirazoline for α_{1A}-AR CHO cells. The rate of acidification of the chamber was calculated by the Cytosoft program (Molecular Devices). Changes in the rate of acidification were calculated as the difference between the maximum effect after agonist addition, and the average of three measurements taken prior to agonist addition. For antagonist studies, a control concentration−response curve was first obtained with clonidine and the cells were then exposed to antagonist for at least 30 min prior to construction of another clonidine concentration−effect curve in the presence of the antagonist. Therefore, each chamber acted as its own control. Data were analyzed as the ability of the antagonist to shift the agonist concentration−effect curve and defined as K_b.

Statistical Analysis. The values of K_i and EC_{50} and the extent of maximal response (E_{max}) were calculated from the computer analysis of binding inhibition data and dose−response curves using the program GraphPad Prism (GraphPad Software, San Diego, CA, USA). The K_b values were calculated as M/concentration ratio^{-1}, where concentration ratio is the EC_{50} obtained in the presence of the antagonist divided by that obtained in the absence of the antagonist.[26] Data were expressed as pK_b [−log10(K_b)] and reported values are means ± SEM of three−six separate experiments.

In Vivo Assays. Animals. Male CD-1 mice (Harlan SRC, Milan, Italy) weighing 25−35 g were used. The mice were kept in a dedicated room, with a 12:12 h light/dark cycle (lights on at 09:00), a temperature of 20 to 22 °C, and a humidity of 45−55%. They were provided with free access to tap water and food pellets (4RF18, Mucedola, Settimo Milanese, Italy). Each mouse was used in only one experimental session. All of the procedures were conducted in adherence to the European Community Directive for the Care and Use of Laboratory Animals. Ethical guidelines for the investigation of experimental pain in conscious animals were followed. The procedures were carried out according to the EEC ethical regulations for animal research (ECC Council 86/609; D. Lgs. 27/01/1992, no. 116), and tests have been approved by the local ethical committee.

Chemicals and Drugs. Morphine hydrochloride was purchased from Salars Spa (Como, Italy) and yohimbine hydrochloride and naloxone hydrochloride from Sigma (St. Louis, MO). Drugs were dissolved in distilled water immediately before use, with the exception of morphine hydrochloride, which was dissolved in saline. Compounds **4**, **5**, and their enantiomers (0.05 mg/kg), yohimbine hydrochloride (1.250 mg/kg) and naloxone (5 mg/kg), were injected intraperitoneally (ip), while morphine hydrochloride was administered subcutaneously (sc) at the dose of 5.0 or 10 mg/kg according to the tests paradigm.

Nociceptive Test. Nociception was evaluated by the radiant heat tail-flick test: briefly, it consists of the irradiation of the lower third of the tail with an IR source (Ugo Basile, Comerio, Italy). The basal predrug latency, ranging between 2 and 3 s, was calculated as the mean of two trials performed at 30 min interval. The mice then received tested drugs or related vehicle 15 min before morphine or saline administration. The antinociceptive activity was evaluated 30, 60, 90, 120, and 240 min after

morphine injection. A cutoff latency of 12 s was established to minimize tissue damage.

To demonstrate the involvement of α_{2C}-AR subtype on the enhancement of morphine antinociception induced by novel compounds, the α_2-AR antagonist yohimbine was administered 15 min before the enantiomers (*S*)-(+)-**4** and (*R*)-(−)-**4**. The antinociceptive effects are expressed as percentage of the maximum possible effect (%MPE), according to the following formula: %MPE = (postdrug latency − baseline latency)/(cutoff value − baseline latency) × 100, where the postdrug latency was the tail-flick latency 30 min after the last morphine dose.

The analgesic effect of morphine (5 mg/kg, sc) was maximal 30 min after administration and then decreased progressively so that it became ineffective 4 h after injection. Pretreatment with (*S*)-(+)-**4** and (*R*)-(−)-**4** induced a rapid (30 min), strong, and long lasting analgesic effect (until 240 min). The overall analysis of variance revealed statistically significant treatment [($F(3.28) = 15.609$; $p < 0.001$] and time effects [($F(4.12) = 30.801$; $p < 0.001$] and interaction time × treatment effects were seen for analgesia latency [($F(12.112) = 2.063$; $p < 0.05$]. Also, pretreatment with (*S*)-(+)-**5** and (*R*)-(−)-**5** significantly increased the morphine-induced antinociception as confirmed by ANOVA [($F(3.28) = 4.043$; $p < 0.05$] (Figure 4A,B). Previous treatment of mice with yohimbine (devoid of analgesic effect when given alone) prevented the increase of morphine analgesia produced by the enantiomers of **4** (Figure 5).

Induction of Morphine Tolerance. In accordance with the literature,[27,28] tolerance was induced in two groups of mice by the injection of morphine (10 mg/kg, sc) twice daily at 12 h intervals for 5 days. Tolerance was evaluated by testing the antinociceptive response to morphine in the tail flick test on the fifth day, 30 min after the last morphine injection. In the experiments on acquisition (development) of morphine tolerance, one group of mice was orally administered with 0.05 mg/kg of **4**, (*S*)-(+)-**4**, and (*R*)-(−)-**4** or vehicle alone, twice daily, 15 min before each morphine treatment. To determinate the effects on the expression phases of morphine tolerance, another group of morphine-treated mice received acute administration of **4**, (*S*)-(+)-**4**, and (*R*)-(−)-**4** (0.05 mg/kg, ip) or vehicle, only 15 min before the last morphine injection on the test day (day 5). The development and expression of morphine tolerance were evaluated by testing the analgesic effects of morphine in the tail-flick test, as previously described.

For morphine tolerance expression, the overall analysis of variance revealed statistically significant treatment [($F(4.41) = 24.499$; $p < 0.001$] and time effects [($F(1.4) = 59.158$; $p < 0.001$] and interaction time × treatment effects were seen for analgesia latency [($F(4.41) = 9.536$; $p < 0.001$]. The mice treated with morphine showed a maximal antinociceptive effect (%MPE) on day 1 ($p < 0.01$) between control and morphine groups. Repeated administration of 10 mg/kg morphine sc twice daily to morphine-treated mice induced a significant decrease in the analgesia latency in the tail-flick test, which resulted in a marked reduction on day 5, as compared with day 1 ($p < 0.01$). Acute administration of **4** or its enantiomers (0.05 mg/kg) 15 min before morphine injection on the test day produced significant decrease in the expression of morphine tolerance, as compared with the morphine vehicle group ($p < 0.01$). The post hoc analysis revealed a statistically significant effect of **4** and (*S*)-(+)-**4** compared to the effect of morphine group on day 5 ($p < 0.01$) and lack of effect for the enantiomer (*R*)-(−)-**4** (Figure 6). Acute administration of **4** and its enantiomers to nondependent mice (control) did not modify the analgesia latency in these mice ($p > 0.05$) (data not shown).

For morphine tolerance development, the overall analysis of variance revealed statistically significant treatment [($F(7.65) = 80.026$; $p < 0.001$] and time effects [($F(1.7) = 70.234$; $p < 0.001$] and interaction time × treatment effects were seen for analgesia latency [($F(7.65) = 11.015$; $p < 0.001$]. The mice treated with morphine showed a maximal antinociceptive effect (%MPE) on day 1 [($F(7.65) = 113.725$; $p < 0.001$]. The post hoc analysis revealed that acute coadministration of **4** or its enantiomers with morphine increased the analgesia on day 1, as compared to related-morphine group on day 1 ($p < 0.01$). Repeated administration of 10 mg/kg morphine sc twice daily to the mice induced a significant decrease in the analgesia latency in the tail-flick test on day 5 [($F(1.15) = 78.275$; $p < 0.001$]. Pretreatment of the mice with **4** or its enantiomers 15 min before each morphine injection inhibited the development of tolerance to morphine analgesia [($F(7.65) = 15.233$; $p < 0.001$]. Finally, repeated administration of **4** or its enantiomers to nondependent mice (Control) did not modify the analgesia latency in these mice ($p < 0.005$) (Figure 9).

Induction of Morphine Dependence. To induce morphine dependence, naïve mice were treated with morphine (10 mg/kg; sc) twice daily at 12 h intervals for 6 days.[27,28] Two hours after the last dose of morphine, the withdrawal syndrome (abstinence), as an index of morphine dependence, was precipitated by an ip injection of naloxone (5 mg/kg).[27,28] The combination of morphine with high dose of naloxone on day 6 has been demonstrated to induce more severe symptoms, including autonomic signs, because naloxone precipitates dose-dependent withdrawal symptoms in animals acutely or chronically dependent upon morphine.[27] Ten minutes before naloxone treatment, the mice were placed in a transparent acrylic cylinder (20 cm diameter, 35 cm high) to habituate them to the new environment. Immediately after the naloxone challenge, each mouse was again placed gently into the cylinder and then monitored for 15 min for the occurrence of withdrawal symptoms (jumping, rearing, forepaw tremor, teeth chatter). To examine the effects on morphine dependence, **4** or its enantiomers were given at dose 0.05 mg/kg ip to one group of mice chronically treated 15 min prior to each morphine injection (acquisition) or to another group of mice acutely treated 15 min before naloxone (expression) as described above. In addition, the effects of **4** or its enantiomers alone on naloxone-induced withdrawal symptoms were examined in nondependent mice, where they received single or repeated administration of these compounds or vehicle. The assessment of naloxone-precipitated withdrawal symptoms after the administration of **4** or its enantiomers has been described above. Repeated administration of morphine produced physical dependence, as assessed by a summary of characteristic set of behavioral responses, which included jumping, rearing, forepaw tremor, and teeth chattering following the naloxone challenge as compared to vehicle ($p < 0.001$). Acute administration of **4**, (*S*)-(+)-**4**, or (*R*)-(−)-**4** 15 min prior to the naloxone injection significantly decreased both the number of jumping, a sign featuring the morphine withdrawal syndrome [($F(4.40) = 15.539$; $p < 0.001$] (Figure 7A), and the frequencies of others withdrawal manifestations, reported as the sum of the frequency of rearing, forepaw tremor, and teeth chattering [($F(4.40) = 16.130$; $p < 0.001$] (Figure 7B) in morphine-dependent mice. No differences were seen for the control mice treated with **4** or its enantiomers as compared with vehicle ($p < 0.05$) (data not shown). Following the naloxone challenge, the mice that received repeated administrations of morphine showed severe signs of withdrawal as compared with the saline control group ($p < 0.01$). Pretreatment of the mice with **4** or its enantiomers 15 min before each morphine injection significantly attenuated both the development of jumping [$F(7.63) = 30.328$; $p < 0.001$] (Figure 10A) and the total signs of withdrawal [$F(7.63) = 41.974$; $p < 0.001$] (Figure 10B). Particularly, jumping was almost completely blocked by **4** because its reduction was 80%. The mice treated with only **4** or its enantiomers (0.05 mg/kg) did not show any significant differences in their withdrawal symptoms, as compared with the control group ($p > 0.05$).

Pentobarbital Sodium-Induced Sleep Time. To rule out a possible sedative effect elicited by (*S*)-(+)-**4** and (*R*)-(−)-**4** as already observed for **4**,[6] these compounds were evaluated on pentobarbital sodium-induced sleep time test. Briefly, groups of mice ($n = 10$) were injected ip with sodium pentobarbital

(50 mg/kg) 15 min after tested compounds (0.05 mg/kg) or vehicle injection. The time between losing and regaining righting reflex (duration of sleeping) was monitored (in seconds) for each animal.[29,30]

All the experiments were replicated independently in separate rounds of animals, and the results were registered by two observers who were blind to the treatment conditions. At tested dose of 0.05 mg/kg, **4** or its enantiomers were not able to increase the sleeping time induced by pentobarbital as compared to control [$F(3.36) = 1.209$, $p < 0.05$] (Figure 8).

Statistical Analysis. The obtained results from the different tests are presented as mean ± SEM. Antinociceptive and morphine tolerance tests were analyzed using two-way split-plot analysis of variance (ANOVA), with treatment as the between-subject factor and time as the within-subject factor; when appropriate, one-way ANOVA was used. The morphine dependence data were analyzed by one-way ANOVA. The differences between groups were determined by a post hoc comparison Newman−Keuls test. Statistical significance was set at $p < 0.05$.

Acknowledgment. We thank the MIUR (Rome), the University of Camerino, and the Fondazione Monte dei Paschi (Siena) for financial support.

Supporting Information Available: Experimental and spectroscopic details of (*S*)-(+)- and (*R*)-(−)-**5**, (*S*)-(+)- and (*R*)-(−)-**6**, (*S*)-(−)-, and (*R*)-(+)-**9**, (*S*)-(+)-, and (*R*)-(−)-**10**, solubility and permeability assays, intrinsic clearance, and elemental analysis of the final compounds. This material is available free of charge via the Internet at http://pubs.acs.org.

References

(1) Part 6 of α_2-Adrenoreceptors profile modulation. For part 5, see ref 6.
(2) Hieble, J. P. Adrenoceptor subclassification: an approach to improved cardiovascular therapeutics. *Pharm. Acta Helv.* **2000**, *74*, 163–171.
(3) Crassous, P.-A.; Denis, C.; Paris, H.; Sénard, J. M. Interest of α_2-adrenergic agonists and antagonists in clinical practice: background, facts and perspectives. *Curr. Top. Med. Chem.* **2007**, *7*, 187–194.
(4) Tan, C. M.; Limbird, L. E. The α_2-adrenergic receptors. In *The Receptors: the Adrenergic Receptors in the 21st Century*; Perez, D., Ed.; Humana Press Inc.: Totowa, NJ, 2006; pp 241−265.
(5) Fairbanks, C. A.; Stone, L. S.; Kitto, K. F.; Nguyen, H. O.; Posthumus, I. J.; Wilcox, G. L. α_{2C}-Adrenergic receptors mediate spinal analgesia and adrenergic-opioid synergy. *J. Pharmacol. Exp. Ther.* **2002**, *300*, 282–290.
(6) Cardinaletti, C.; Mattioli, L.; Ghelfi, F.; Del Bello, F.; Giannella, M.; Bruzzone, A.; Paris, H.; Perfumi, M.; Piergentili, A.; Quaglia, W.; Pigini, M. Might adrenergic α_{2C}-agonists/α_{2A}antagonists become novel therapeutic tools for pain treatment with morphine? *J. Med. Chem.* **2009**, *52*, 7319–7322 and references therein.
(7) Gentili, F.; Bousquet, P.; Brasili, L.; Caretto, M.; Carrieri, A.; Dontenwill, M.; Giannella, M.; Marucci, G.; Perfumi, M.; Piergentili, A.; Quaglia, W.; Rascente, C.; Pigini, M. α_2-Adrenoreceptors profile modulation and high antinociceptive activity of (*S*)-(−)2-[1-biphenyl-2-yloxy]ethyl]-4,5-dihydro-1*H*-imidazole. *J. Med. Chem.* **2002**, *45*, 32–40.
(8) Gentili, F.; Ghelfi, F.; Giannella, M.; Piergentili, A.; Pigini, M.; Quaglia, W.; Vesprini, C.; Crassous, P.-A.; Paris, H.; Carrieri, A. α_2-Adrenoreceptors profile modulation. 2. Biphenyline analogues as tools for selective activation of the α_{2C}-subtype. *J. Med. Chem.* **2004**, *47*, 6160–6173.
(9) Shi, L.; Javitch, J. A. The binding site of aminergic G protein-coupled receptors: the transmembrane segments and second extracellular loop. *Annu. Rev. Pharmacol. Toxicol.* **2002**, *42*, 437–467.
(10) Gentili, F.; Cardinaletti, C.; Vesprini, C.; Carrieri, A.; Ghelfi, F.; Farande, A.; Giannella, M.; Piergentili, A.; Quaglia, W.; Laurila, J. M.; Huhtinen, A.; Scheinin, M.; Pigini, M. α_2-Adrenoreceptors profile modulation. 4. From antagonist to agonist behaviour. *J. Med. Chem.* **2008**, *51*, 4289–4299.
(11) Crassous, P.-A.; Cardinaletti, C.; Carrieri, A.; Bruni, B.; Di Vaira, M.; Gentili, F.; Ghelfi, F.; Giannella, M.; Paris, H.; Piergentili, A.; Quaglia, W.; Schaak, S.; Vesprini, C.; Pigini, M. α_2-Adrenoreceptors profile modulation. 3. (*R*)-(+)-*m*-Nitrobiphenyline, a new efficient and α_{2C}-subtype selective agonist. *J. Med. Chem.* **2007**, *50*, 3964–3968.
(12) Arredondo, Y.; Moreno-Mañas, M.; Pleixats, R.; Palacin, C.; Raga, M. M.; Castelló, J. M.; Ortiz, J. A. Preparation, antimicrobial evaluation, and mutagenicity of [2-hydroxyaryl]-[1-methyl-5-nitro-1*H*-2-imidazolyl]methanols, [5-*tert*-butyl-2-methylaminophenyl]-[1-methyl-5-nitro-1*H*-2 imidazolyl]methanol, and [2-hydroxyaryl]-[1-methyl-5-nitro-1*H*-2-imidazolyl] ketones. *Bioorg. Med. Chem.* **1997**, *5*, 1959–1968.
(13) Bishop, M. J.; Barvian, K. A.; Berman, J.; Bigham, E. C.; Garrison, D. T.; Gobel, M. J.; Hodson, S. J.; Irving, P. E.; Liacos, J. A.; Navas, I.; Saussy, D. L.; Speake, J. D. α_1-Adrenoceptor agonists: the identification of novel α_{1A} subtype selective 2′-heteroaryl-2-(phenoxymethyl)imidazolines. *Bioorg. Med. Chem. Lett.* **2002**, *3*, 471–475.
(14) Tottie, L.; Baeckström, P.; Moberg, C.; Tegenfeldt, J.; Heumann, A. Molecular sieve controlled diastereoselectivity: effect in the palladium-catalyzed cyclization of *cis*-1,2-divinylcyclohexane with R-oxygen-substituted acids as chiral nucleophiles. *J. Org. Chem.* **1992**, *57*, 6579–6587.
(15) Boström, J.; Hogner, A.; Schmitt, S. Do structurally similar ligands bind in a similar fashion? *J. Med. Chem.* **2006**, *49*, 6716–6725.
(16) Özdoğan, U. K.; Lähdesmäki, J.; Scheinin, M. Influence of prazosin and clonidine on morphine analgesia, tolerance and withdrawal in mice. *Eur. J. Pharmacol.* **2003**, *460*, 127–134.
(17) Özdoğan, U. K.; Lähdesmäki, J.; Hakala, K.; Scheinin, M. The involvement of α_{2A}-adrenoceptors in morphine analgesia, tolerance and withdrawal in mice. *Eur. J. Pharmacol.* **2004**, *497*, 161–171.
(18) Koob, G. F.; Le Moal, M. Neurobiological mechanisms for opponent motivational processes in addiction. *Philos. Trans. R. Soc., B* **2008**, *363*, 3113–3123.
(19) Di, L.; Kerns, E. H.; Fan, K.; McConnell, O. J.; Carter, G. T. High throughput artificial membrane permeability assay for blood−brain barrier. *Eur. J. Med. Chem.* **2003**, *38*, 223–232.
(20) Gowing, L.; Farrell, M.; Ali, R.; White, J. M. Alpha2 adrenergic agonists for the management of opioid withdrawal. *Cochrane Database Syst. Rev.* **2009**, *2*, CD002024.
(21) Veilleux, J. C.; Colvin, P. J.; Anderson, J.; York, C.; Heinz, A. J. A review of opioid dependence treatment: pharmacological and psychosocial interventions to treat opioid addiction. *Clin. Psychol. Rev.* **2010**, *30*, 155–166.
(22) El-Kadi, A. O.; Sharif, S. I. The influence of chronic treatment with clonidine, yohimbine and idazoxan on morphine withdrawal. *Psychopharmacology* **1997**, *132*, 67–73.
(23) Hameedi, F. A.; Woods, S. W.; Rosen, M. I.; Pearsall, H. R.; Kosten, T. R. Dose dependent effects of yohimbine on methadone maintained patients. *Am. J. Drug Alcohol Abuse* **1997**, *23*, 327–333.
(24) Schaak, S.; Devedjian, J. C.; Paris, H. Use of eukaryotic vectors for the expression of adrenergic receptors. *Methods Mol. Biol.* **2000**, *126*, 189–206.
(25) Testa, R.; Taddei, C.; Poggesi, E.; Destefani, C.; Cotecchia, S.; Hieble, J. P.; Sulpizio, A. C.; Naselsky, D.; Bergsma, D.; Ellis, S.; Swift, A.; Ganguly, S.; Ruffolo, R. R.; Leonardi, A. Rec 15/2739 (SB 216469): a Novel prostate selective α_1-adrenoceptor antagonist. *Pharmacol. Commun.* **1995**, *6*, 79–86.
(26) Arunlakshana, O.; Schild, H. O. Some quantitative uses of drug antagonists. *Br. J. Pharmacol. Chemother.* **1959**, *14*, 48–58.
(27) Ren, X.; Noda, Y.; Mamiya, T.; Nagai, T.; Nabeshima, T. A neuroactive steroid, dehydroepiandrosterone sulfate, prevents the development of morphine dependence and tolerance via c-fos expression linked to the extracellular signal-regulated protein kinase. *Behav. Brain Res.* **2004**, *152*, 243–250.
(28) Abdel-Zaher, A. O.; Hamdy, M. M.; Aly, S. A.; Abdel-Hady, R. H.; Abdel-Rahman, S. Attenuation of morphine tolerance and dependence by aminoguanidine in mice. *Eur. J. Pharmacol.* **2006**, *540*, 60–66.
(29) Carvalho, A. A.; Galdino, P. M.; Nascimento, M. V.; Kato, M. J.; Valadares, M. C.; Cunha, L. C.; Costa, E. A. Antinociceptive and antiinflammatory activities of grandisin extracted from *Virola surinamensis*. *Phytother. Res.* **2010**, *24*, 113–118.
(30) Carlini, E. A.; Burgos, V. Screening farmacológico de ansiolíticos: metodologia laboratorial e comparação entre diazepam e clorobenzepam. *Rev. Assoc. Bras. Psiq.* **1979**, *1*, 25–31.